Effects of Organically Modified Nanoclay on the Transport Properties and Electrochemical Performance of Acid-Doped Polybenzimidazole Membranes

Mohammad Mahdi Hasani-Sadrabadi,[1,2] Nassir Mokarram Dorri,[3] Seyed Reza Ghaffarian,[1] Erfan Dashtimoghadam,[1] Kaveh Sarikhani,[1] Fatemeh S. Majedi[2]

[1]*Polymer Engineering Department, Amirkabir University of Technology, Tehran, Iran*
[2]*Biomedical Engineering Department, Amirkabir University of Technology, Tehran, Iran*
[3]*School of Polymer, Textile and Fiber Engineering, Georgia Institute of Technology, Atlanta, Georgia*

Received 14 March 2009; accepted 13 December 2009
DOI 10.1002/app.31974
Published online 26 March 2010 in Wiley InterScience (www.interscience.wiley.com).

ABSTRACT: Nanocomposite polyelectrolyte membranes based on phosphoric acid (H_3PO_4) doped polybenzimidazoles (PBIs) with various loading weights of organically modified montmorillonite (OMMT) were prepared and characterized for direct methanol fuel cell (DMFC) applications. X-ray diffraction analysis revealed the exfoliated structure of OMMT nanolayers in the polymeric matrices. An H_3PO_4–PBI/OMMT membrane composed of 500 mol % doped acid and 3.0 wt % OMMT showed a membrane selectivity of approximately 109,761 in comparison with 40,500 for Nafion 117 and also a higher power density (186 mW/cm^2) than Nafion 117 (108 mW/cm^2) for a single-cell DMFC at a 5*M* methanol feed. © 2010 Wiley Periodicals, Inc. J Appl Polym Sci 117: 1227–1233, 2010

Key words: clay; functionalization of polymers; ionomers; membranes; nanocomposites

INTRODUCTION

Fuel cells have emerged as efficient energy-conversion devices for reducing the demands for fossil fuel and nuclear-derived energy, both in the power-generation sector and the road-transport sector.[1] Unlike conventional power-generation technologies, fuel cells operate without combustion and, consequently, have minimal environmental side effects.[2]

Direct methanol fuel cells (DMFCs) are one of the most promising systems for various applications where both high efficiency and low weight are required.[3] Methanol is an easily handled liquid, has limited toxicity, and has a high energy density (3800 kcal/L) compared to H_2 (658 kcal/L).[4] The desired DMFC half-reactions are as follows:[5]

$$CH_3OH + H_2O \longrightarrow CO_2 + 6H^+ + 6e^-$$

$$1.5O_2 + 6H^+ + 6e^- \longrightarrow 3H_2O$$

Available DMFC technology suffers from two major limitations, which are the poor oxidation kinetics of the fuel and the permeation of methanol into the cathode.[6–10] The high rate of methanol permeation through a polymer electrolyte membrane results in a loss of fuel-cell efficiency through the chemical reaction of the fuel with oxygen and the depolarization of the cathode.[11]

Nafion, a perfluorosulfonated membrane from DuPont, has been intensively used in fuel cells as a solid electrolyte. Although Nafion membranes combine mechanical strength and chemical/thermal stability with high proton conductivity,[12,13] their drawbacks, including a high cost, high methanol permeability, and low conductivity at elevated temperatures, have limited their widespread application in DMFCs.[14] Hence, many researches have dedicated their time to the development of alternative proton-exchange membranes (PEMs).

PEMs are a key component in polymeric electrolyte fuel cells, which provide communications of protons between the anode and cathode and act as a fuel separator.[15] To reduce the methanol crossover of the membranes at medium operational temperatures (150–200°C), new and more selective materials are required. Ideal membranes for DMFCs should not only conduct protons but also act as a fuel barrier. Different approaches have been used to reduce the methanol permeability so far: passive approaches, such as use of diluted methanol and operation at low temperatures, which affect DMFC performance adversely,[16] and active approaches, such as the modification of

Correspondence to: S. R. Ghaffarian (sr_ghaffarian@aut.ac.ir).

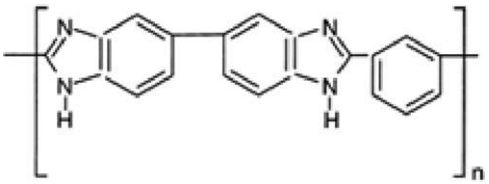

Scheme 1 Poly[2,2′-(*m*-phenylene)-5,5′-bibenzimidazole].

membranes through the incorporation of inorganic components.[5,17–28]

Aromatic polybenzimidazoles (PBIs) are highly thermostable polymers with melting points over 600°C. The commercially available PBI is poly[2,2′-(*m*-phenylene)-5,5′-bibenzimidazole] (Scheme 1), which is synthesized from diphenyl isophthalate and tetraaminobiphenyl.[29] The systematic study of the complexation of PBI with phosphoric acid (H_3PO_4) to provide thermooxidatively stable proton-conducting membranes for fuel cell applications began in 1994.[30] Generally, two routes have been developed to improve the proton-conduction properties: complexation with acids and the grafting of functional groups onto PBI. Such possible reactions are due to the particular reactivity of PBI and arise from the —N= and —NH groups of the imidazole ring. Moreover, because of its basic character ($pK_a \sim 5.5$), PBI complexes with inorganic and organic acids.[30,31] The —NH groups in the PBI structure are reactive, so hydrogen can be abstracted, and functional groups can then be grafted onto the anionic polymer backbone.[32,33]

The main objective of this study was to provide a PEM with a low fuel permeability rate and a high proton conductivity. Hence, nanocomposite membranes based on H_3PO_4-doped PBI and organically modified montmorillonite (OMMT) were fabricated, and their transport properties and electrochemical performance were compared with Nafion 117 as a commercial membrane.

EXPERIMENTAL

Materials and methods

In the first step, PBI (Celazole, Hoechst Celanese, Bridgewater, NJ), *N,N*-dimethylacetamide (DMAc; Merck, Darmstadt, Germany), and lithium chloride (LiCl; Merck), were placed in a high-pressure reactor with a nitrogen atmosphere and heated to 250°C under 100 psi pressure for 5 h. After the solution cooled, it was filtered and mixed with a suspension of organically treated montmorillonite clay (OMMT, Cloisite 15A, from Southern Clay Products, Inc., Gonzales, TX) at 0.5, 1.0, 1.5, 3.0, 5.0, and 10.0 wt %. OMMT was suspended in DMAc at room temperature, stirred for 2 h, and ultrasonicated for another hour. The resultant polymeric mixtures were ultrasonicated for another 30 min, stirred at 80°C for 8 h, and concentrated by means of a rotary evaporator to a viscosity suitable for film casting. Afterward, the mixtures were cast onto glass plates and dried in a vacuum oven at 70°C overnight to remove the solvent. Then, the films were washed twice in boiling water (to remove any remaining solvent and LiCl) and dried. Finally, the PBI-based membranes were doped through immersion in 11*M* aqueous H_3PO_4 (Merck) for a week to provide about 500 mol % acid doping.

Deionized water (purified with a Milli-Q Academic System) was used in this study. The catalysts, platinum black for the cathode and platinum–ruthenium black for the anode, were purchased from Johnson–Matthey (London, UK). Nafion 117 membranes with thicknesses of 178 μm and a Nafion 5 wt % solution were acquired from DuPont Co. (Wilmington, DE) and were used to compare the data and membrane electrode assembly (MEA), respectively.

The PBI-based membranes before use were boiled in deionized water for 1 h and were then washed several times. As membrane treatment, the Nafion membranes were boiled in hydrogen peroxide (3% v/v, 30 min), washed several times with deionized water, and boiled for 1 h in deionized water. The Nafion membranes were then boiled in sulfuric acid (0.5*M*) for another hour and washed several times.

The MEAs were prepared by catalyst decaling and painting methods[34,35] similar to those presented in our previous reports.[22,24–28] Platinum black and platinum–ruthenium black were used as catalysts for the anode and cathode, respectively. The catalysts were mixed with a 5 wt % Nafion solution (as a binder) and several drops of glycerol (a suspension/painting agent). Dilute Nafion solution is a common binder in the fabrication of perfect MEAs. In this study, a similar method was used to prepare MEAs based on both PBI and Nafion membranes. As reported previously,[36] the sulfonate groups of Nafion and benzimidazole groups of PBI provide acid–base interaction, which results in a strong and stable structure. The PBI-based membranes were washed after MEA fabrication and then stored in deionized water for further application.

Subsequently, the resulting suspension (4 mg/cm^2) was brushed directly onto the dry membranes (3 × 3 cm^2) and hot-pressed (200 kg/cm^2) at 120°C for 90 s on each membrane side to increase the contact area between the catalyst layer and membranes.

Characterization

The dispersion of clay particles in the membranes was analyzed by X-ray diffraction (XRD; XRD-D5000

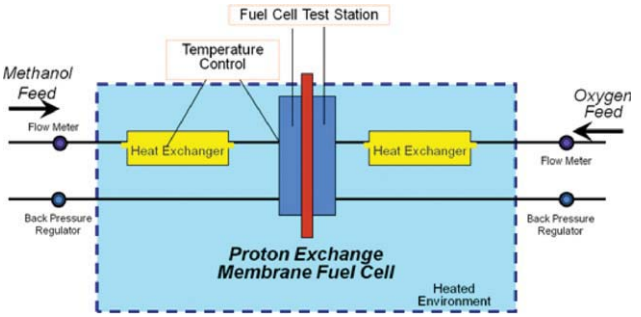

Figure 1 Schematic diagram of the DMFC test system. [Color figure can be viewed in the online issue, which is available at www.interscience.wiley.com.]

diffractometer Cu Kα, Siemens, Madison, WI). The scanning diffraction angle (2θ) was between 2 and 15°.

The proton conductivity of fully hydrated membranes was measured at different temperatures with the four-point probe method. The conductivity values were calculated as follows:

$$\text{Conductivity} = LR^{-1}A^{-1}$$

where L is the distance between the reference electrodes, A is the cross-sectional area of the membrane sample, and R is the resistance. Alternating-current impedance measurements for resistance evaluation were made with a Solartron Interface 1260 (Hampshire, UK) gain phase analyzer over the frequency range 1–10^6 Hz. In addition, to evaluate the temperature dependency of proton conductivities, conductivity measurements were performed in the temperature range 25–70°C.

The methanol diffusion coefficient (DK) was measured by means of a laboratory-made, two-compartment glass diffusion cell. One side of the diffusion cell (cell A) was filled with a methanol solution, and pure water was placed on the other side (cell B). The solution in each compartment was continuously stirred to ensure uniformity. The concentration of the methanol in cell B was measured by a gas chromatography method. DK (cm^2/s) was determined as follows:

$$C_{B(t)} = \frac{A}{V_B}\frac{\text{DK}}{L}C(t - t_0)$$

where $C_{B(t)}$ is the concentration of methanol in cell B (mol/L), C is the methanol concentration in cell A (mol/L), V_B is the volume of diffusion reservoir (cm^3), A is the membrane area (cm^2), L is the membrane thickness (cm), t is the time of measurement (s), and t_0 is the initial time (s).

The DMFC single cell was made from four 316 stainless steel plates (end plates and flow fields), two carbon papers (gas diffusion layers; TGP-H-120, Toray, Tokyo, Japan), and an MEA. Silicon rubber sheets were used to seal internal sections. The performance of the single cell was evaluated at two methanol concentrations (1 and 5*M*) and with oxygen flow in the anode and cathode sides at 70°C. Methanol was fed to the anode side at 20 psi back pressure for 1 h, and oxygen was introduced to the cathode side with a gradual pressure increase to 20 psi. The single cell was allowed to run for 0.5 h before data collection of the polarization curves. All single-cell tests were conducted three times, and the obtained results are presented as average values. The schematic diagram of the fuel-cell testing apparatus is illustrated in Figure 1.

RESULTS AND DISCUSSION

To obtain high-performance membranes for DMFC applications, the methanol permeability should be reduced as much as possible. It has been suggested that a significant reduction in methanol crossover could be achieved through the modification of the size of the proton-transport nanochannels and the introduction of zigzag pathways against methanol.[21–28] In this respect, OMMT was incorporated into the PBI matrices in the current study. XRD analysis was used to study the microstructure of the prepared nanocomposite membranes. The XRD patterns of the OMMT, PBI, and PBI/OMMT-3 wt % nanocomposite membrane are illustrated in Figure 2. By monitoring the position, shape, and intensity of the basal reflections from the distributed silicate layers, we could identify the nanocomposite structure (intercalated or exfoliated). The intercalation of the polymer chains usually increased the interlayer spacing of OMMT. In an exfoliated nanocomposite,

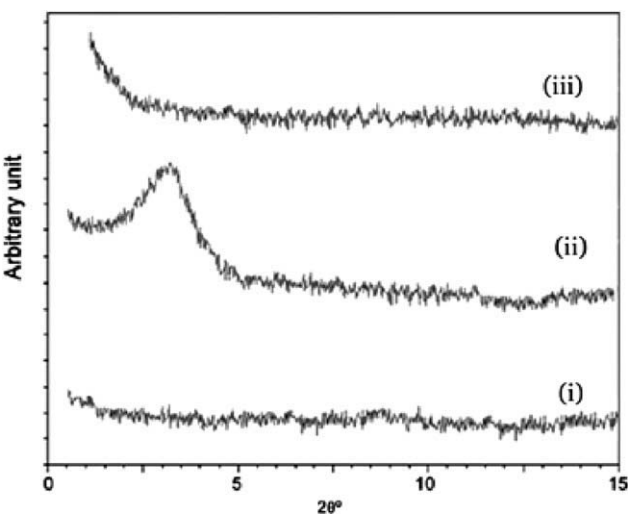

Figure 2 XRD patterns of (i) PBI, (ii) OMMT, and (iii) the PBI/OMMT-3 wt % nanocomposite membrane.

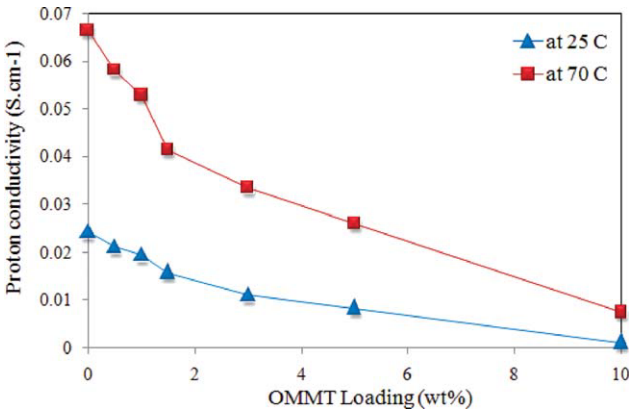

Figure 3 Proton conductivity of the nanocomposite membranes based on PBI filled with various contents of OMMT at 25 and 70°C. [Color figure can be viewed in the online issue, which is available at www.interscience.wiley.com.]

the extensive layer separation associated with the delamination of the original silicate layers in the polymer matrix results in the eventual disappearance of any coherent XRD from the distributed silicate layers.[37,38] As shown in Figure 2, OMMT showed one crystalline peak around 3°. However, this peak almost disappeared in the case of the PBI/OMMT nanocomposite, which was due to the diffusion of the PBI chains into the crystalline parts of OMMT particles and provided exfoliated composite membranes.

The effects of the OMMT particle loading on the proton conductivity and methanol permeability of the PBI nanocomposite membranes are shown in Figures 3 and 4, respectively. The proton conductivity and methanol permeability of the PBI-based membranes were measured to be approximately 0.001 S/cm and 4.36 $\times$ 10^{-8} cm^2/s, respectively, for 10% OMMT and about 0.011 S/cm and 1.0 $\times$ 10^{-7} cm^2/s, respectively, for 3% OMMT. As a well-known effect, the presence of impermeable OMMT sheets introduced tortuous pathways against penetrating molecules. In other words, the reduction of methanol permeability arose from the longer diffusive routes of methanol molecules in the presence of nanoclay in comparison with the pristine PBI matrix. On the other hand, such an effect also hindered the proton conduction, and the hydrophobic nature of the organically treated OMMT particles led to a decrease in the proton-conductivity values (Fig. 3). The proton conductivities of the PBI membranes were measured to be 0.0663 S/cm for the unfilled membrane and 0.0333 S/cm for the 3 wt % OMMT membrane. Moreover, the proton-conductivity values of the nanocomposite membranes at a temperature of 70°C are also shown in Figure 3. As seen, the PBI-based membranes provided higher conductivity at 70°C, which suggested the H_3PO_4-doped PBI membrane to be one of the most promising polyelectrolytes for PEM fuel-cell applications at elevated temperatures.[39]

Proton conductivity and methanol permeability are the two transport properties of a PEM that have a significant effect on the performance of the corresponding DMFC. As discussed before, the presence of OMMT has a favorable influence on the methanol permeability and an adverse effect on the proton conductivity. The *selectivity parameter*, which is defined as the ratio of proton conductivity to methanol permeability, is often used to evaluate the potential performance of PEMs for DMFC applications.[21–28] Because the higher selectivity value leads to better membrane performance under DMFC operational

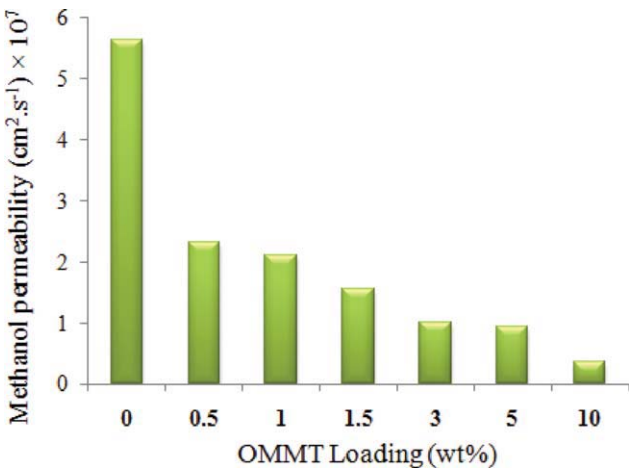

Figure 4 Effect of the particle loading weight on the methanol permeability of the acid-doped, PBI-based nanocomposite membranes. [Color figure can be viewed in the online issue, which is available at www.interscience.wiley.com.]

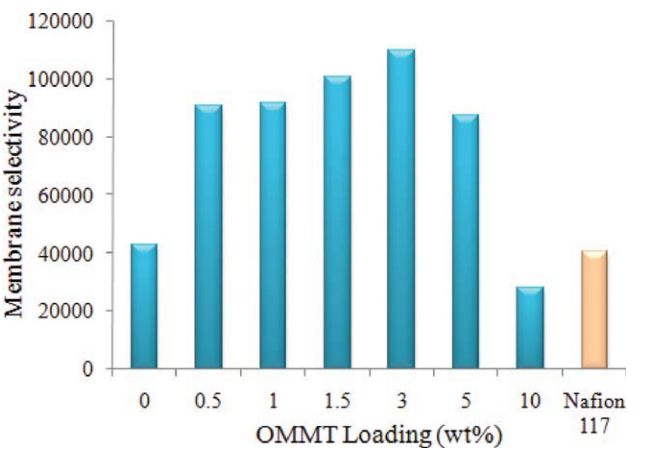

Figure 5 Membrane selectivity of the PBI-based nanocomposite membranes with different OMMT loading weights at 25°C. [Color figure can be viewed in the online issue, which is available at www.interscience.wiley.com.]

TABLE I
Comparison of the Parameters for Various DMFC Membranes

PEM	Proton conductivity (S/cm)[a,b]	Methanol permeability ($\times 10^6$ cm^2/s)[b]	Membrane selectivity	Reference
H_3PO_4-doped PBI (500 mol %) + 3% OMMT	0.0173	0.1	109,800	This study
Sulfonated PEEK (62% sulfonation) + 1% OMMT	0.011	0.205	84,400	21
Sulfonated PPO (27% sulfonation) + 2% OMMT	0.0108	0.17	63,500	22
Nafion 117	0.081	2.00	40,500	This study
Tetrafluoroethylene with poly(styrene sulfonic acid)[c]				
Pall R1010 (36 μm)	0.08	6	13,350	14 and 22
Pall R4010 (63 μm)	0.072	4.2	17,500	

PEEK = poly(ether ether ketone); PPO = poly(propylene oxide).
[a] Along the plane of the membrane
[b] Measured at room temperature.
[c] Pall Gelman Sciences (Washington, NY).

conditions, more selective membranes are more preferable for DMFC applications.

The selectivity values of the acid-doped PBI and corresponding nanocomposite membranes at various OMMT contents are shown in Figure 5. As illustrated, a remarkable improvement in the membrane selectivity was achieved with the incorporation of OMMT into the PBI matrices. Although with increasing OMMT loading either the proton conductivity or methanol permeability decreased, the reduction rate of methanol permeability was higher than proton conductivity. Accordingly, the selectivity parameter was improved to reach its optimum (maximum) value. Among the H_3PO_4–PBI/OMMT nanocomposite membranes, a maximum selectivity value of about 109,761 appeared at 3.0 wt % OMMT compared to that of 40,500 for the Nafion 117 membrane. At higher OMMT contents, because of the very low proton-conductivity values, the membrane selectivity diminished remarkably. The proton-conductivity, methanol permeability, and membrane selectivity properties of the various DMFC membranes are summarized in Table I, which indicates the highest selectivity value for acid-doped PBI comprising 3% OMMT compared to the other membranes.

As mentioned, the PBI-based membranes were washed after MEA fabrication and then stored in deionized water for further processing. The interaction between the positive groups of PBI and the negative groups of H_3PO_4 was too strong, and as a result, the doping of PBI was stable even under harsh conditions, so through the washing process, the level of doped acid did not change significantly.[39] A DMFC single-cell performance test was performed, and the plots of cell potential (polarization curves) and power density versus current density for the manufactured DMFC at two different methanol concentrations (1 and 5*M*) at 70°C are shown in Figure 6. The current densities for the acid-doped PBI membrane (at 500 mol % acid doping), PBI-based nanocomposite membranes (at 500 mol % acid doping and 3.0 wt % OMMT loading), and Nafion 117, were measured to be 290, 260, and 351 mA/cm^2 at a potential of 0.2 V and 1*M* methanol feed and 635, 723, and 420 mA/cm^2 at a 0.2-V potential and 5*M* methanol concentration,

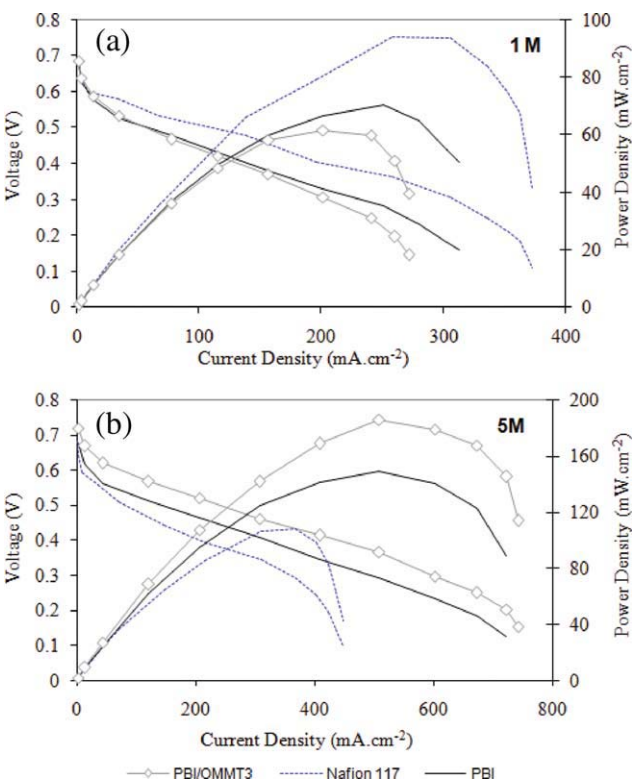

Figure 6 Polarization curves of DMFC single cells consisting of PBI, PBI/OMMT nanocomposite membranes, and Nafion 117. The single cell test was performed with (a) a 1*M* methanol solution or (b) a 5*M* methanol solution with 20 psi of pressure for the anode and oxygen with 20 psi of pressure for the cathode at 70°C. [Color figure can be viewed in the online issue, which is available at www.interscience.wiley.com.]

respectively. The power densities for the acid-doped PBI, H_3PO_4–PBI/3.0 wt % OMMT, and Nafion 117 were obtained as 59, 51, and 77 mW/cm^2, respectively, at a potential of 0.2 V and a methanol concentration of 1*M* and 130, 145, and 83 mW/cm^2, respectively, at a potential of 0.2 V and a methanol concentration of 5*M*. Moreover, the maximum power densities for the H_3PO_4–PBI, H_3PO_4–PBI/3.0 wt % OMMT, and Nafion membranes were 70, 62, and 94 mW/cm^2, respectively, at a 1*M* methanol concentration and 149, 186, and 108 mW/cm^2, respectively, at a 5*M* methanol concentration.

The open-circuit voltage (OCV) of the DMFC for the H_3PO_4-doped PBI, H_3PO_4–PBI/3.0 wt % OMMT, and Nafion 117 were measured to be 0.675, 0.685, and 0.69, respectively, for 1*M* methanol and 0.675, 0.718, and 0.66, respectively, for 5*M* methanol. OCV is in close relation with the methanol crossover, and a higher OCV value is considered to be an indication of lower methanol crossover.[22,24–28] The obtained OCV values revealed the superiority of the pristine and nanocomposite PBI-based membranes at a concentrated methanol feed (5*M*) to the Nafion 117. The higher OCV clearly indicated that OMMT incorporated into the PBI matrix had truly decreased the rate of methanol crossover. Moreover, the nanocomposite membrane showed a higher power density than Nafion 117 and unfilled PBI at a higher methanol concentration. The higher performance of Nafion 117 at a 1*M* methanol feed was due to its higher conductivity, despite its higher methanol permeability. Under the conditions of a more concentrated methanol feed (5*M*), the adverse effect of methanol permeability prevailed and resulted in a remarkable reduction of performance. The electro-osmotic contribution became more important when the electric current increased, which depended on the methanol concentration of the feed solution. Although performance testing was not done at higher temperatures (>100°C), the results of the DMFC single-cell test revealed the superiority of the PBI-based nanocomposite membranes, even at 70°C. Because conductivity is a temperature-activated process,[27] we expected that the conductivity of the PBI-based membranes would increase at higher temperatures. On the other hand, the methanol permeability of the Nafion-based membrane increased with increasing temperature and decreased the performance of the corresponding DMFC, which was confirmed with polarization curves, as shown in Figure 6. Moreover, from Figure 6, we found that the PBI nanocomposite membranes were able to provide a higher power density at a concentrated methanol feed (5*M*) than Nafion 117, which was due to the reduced methanol crossover in the presence of OMMT nanolayers. Hence, one could expect that PBI-based nanocomposite membranes would provide a higher power density also at higher temperatures, and their superiority to Nafion, even at lower temperatures, indicates their broader operational temperature ranges. In accordance with the results of the DMFC single cell, we expect that the prepared nanocomposite membranes to be promising for DMFC applications.

CONCLUSIONS

In this study, H_3PO_4-doped PBI-based nanocomposite membranes composed of different amounts of OMMT were prepared. We found that the fabricated nanocomposite membranes fulfilled advantageous properties, including high proton conductivity (up to 2.1×10^{-2} S/cm), low methanol permeability (down to 4.36×10^{-8} cm^2/s), and also convenient processability. The membrane selectivity parameters of the PBI-based composite and Nafion 117 were calculated when the OMMT loading was less than 10 wt %. The nanocomposite membrane with 3 wt % OMMT was able to provide a higher selectivity and power density at a concentrated methanol feed of 5*M* compared to the Nafion 117 membrane. The composite membranes were easy to prepare and much less expensive than commercial perfluorinated membranes, such as Nafion. Because of the several favorable properties of high proton conductivity, low methanol permeability, high power density, ease of preparation, and low cost, acid-doped PBI/OMMT nanocomposite membranes could be considered as promising alternatives of perfluorosulfonated membranes for DMFC applications.

References

1. Jones, D. J.; Rozière, J. J Membr Sci 2001, 185, 41.
2. Vielstich, W.; Lamm, A.; Gasteiger, H. A. Handbook of Fuel Cells: Fundamentals, Technology, and Applications; Wiley: Chichester, United Kingdom, 2003; Vol. 1.
3. Song, M. K.; Park, S. B.; Kim, Y. T.; Kim, K. H.; Min, S. K.; Rhee, H. W. Electrochim Acta 2004, 50, 639.
4. Gurau, B.; Smotkin, E. S. J Power Sources 2002, 112, 339.
5. Rivera, H.; Lawton, J. S.; Budil, D. E.; Smotkin, E. S. J Phys Chem B 2008, 112, 8542.
6. Arico, A. S.; Srinivasan, S.; Antonucci, V. Fuel Cells 2001, 1, 133.
7. Silva, V. S.; Weisshaar, S.; Reissner, R.; Ruffmann, B.; Vetter, S.; Mendes, A.; Madeira, L. M.; Nunes, S. J Power Sources 2005, 145, 485.
8. Jörissen, L.; Gogel, V.; Kerres, J.; Garche, J. J Power Sources 2002, 105, 267.
9. Peluca, N. W.; Elabd, Y. A. J Polym Sci Part B: Polym Phys 2006, 44, 2201.
10. Lobato, J.; Canizares, P.; Rodrigo, M. A.; Linares, J. J.; Vizcaino, R. L. Energy Fuels 2008, 22, 3335.
11. Savinell, R.; Yeager, E.; Tryk, D.; Landau, U.; Wainright, J.; Weng, D.; Lux, K.; Litt, M.; Rogers, C. J Electrochem Soc 1994, 141, 46.

12. Ren, X.; Zelenay, P.; Thomas, S.; Davey, J.; Gottesfeld, S. J Power Sources 2000, 86, 111.
13. Savadogo, O. J. New Mater Electrochem Syst 1998, 1, 47.
14. Neburchilov, V.; Martin, J.; Wang, H.; Zhang, J. J Power Sources 2007, 169, 221.
15. Kreuer, K. D. J Membr Sci 2001, 185, 29.
16. Kalhammer, F. R.; Prokopius, P. R.; Roan, V. P.; Voecks, G. E. Status and Prospects of Fuel Cells as Automobile Engines: A Report of the Fuel Cell Technical Advisory Panel, July 1998. http://www.arb.ca.gov/h2fuelcell/kalhammer/techreport/execsum.pdf (accessed Dec 2009).
17. Reichert, P.; Kressler, J.; Thomann, R.; Mulhaupt, R.; Stoppelmann, G. Acta Polym 1998, 4911, 116.
18. Giannellis, E. P. Appl Organomet Chem 1998, 12, 675.
19. Lin, Y. F.; Yen, C. Y.; Ma, C. C. M.; Liao, S. H.; Hung, Y. H.; Hsiao, Y. H. J Power Sources 2007, 165, 692.
20. Stangar, U. L.; Groselj, N.; Orel, B.; Schmitz, A.; Colomban, P. Solid State Ionics 2001, 145, 109.
21. Hasani-Sadrabadi, M. M.; Emami, S. H.; Ghaffarian, S. R.; Moaddel, H. Energy Fuels 2008, 22, 2539.
22. Hasani-Sadrabadi, M. M.; Emami, S. H.; Moaddel, H. J Power Sources 2008, 183, 551.
23. Hasani-Sadrabadi, M. M.; Dashtimoghadam, E.; Majedi, F. S.; Kabiri, K. J Power Sources 2009, 190, 318.
24. Hasani-Sadrabadi, M. M.; Dashtimoghadam, E.; Ghaffarian, S. R. ECS Trans 2009, 17, 269.
25. Hasani-Sadrabadi, M. M.; Dashtimoghadam, E.; Ghaffarian, S. R.; Hasani-Sadrabadi, M. H.; Heidari, M.; Moaddel, H. Renewable Energy 2010, 35, 226.
26. Dashtimoghadam, E.; Hasani-Sadrabadi, M. M.; Moaddel, H. Polym Adv Technol, to appear.
27. Hasani-Sadrabadi, M. M.; Ghaffarian, S. R.; Mokarram-Dorri, N.; Dashtimoghadam, E.; Majedi, F. S. Solid State Ionics 2009, 180, 1497.
28. Hasani-Sadrabadi, M. M.; Dashtimoghadam, E.; Sarikhani, K.; Majedi, F. S.; Khanbabaei, G. J Power Sources 2010, 195, 2450.
29. Vogel, H.; Marvel, C. S. J Polym Sci 1961, 50, 511.
30. Wainright, J. S.; Wang, J.-T.; Savinell, R. F.; Litt, M.; Moaddel, H.; Rogers, C. Proc Electrochem Soc 1994, 94, 255.
31. Wainright, J. S.; Savinell, R. F.; Litt, M. H. Proc Int Symp New Mater Fuel Cell Mod Battery Syst 1997, 2, 808.
32. Preston, P. M.; Smith, D. M.; Tennant, G. Benzimidazoles and Congeneric Tricyclic Compounds Part I; Wiley: New York, 1981.
33. Sansone, M. J. U.S. Pat. 4,898,917 (1990).
34. Gottesfeld, S.; Wilson, M. J Electrochem Soc 1992, 139, L28.
35. Gottesfeld, S.; Zawodzinski, T. Adv Electrochem Sci Eng 1997, 5, 195.
36. Wycisk, R.; Chisholm, J.; Lee, J.; Lin, J.; Pintauro, P. N. J Power Sources 2006, 163, 9.
37. Sinha Ray, S.; Okamoto, M. Prog Polym Sci 2003, 28, 1539.
38. Chisholm, B. J.; Moore, R. B.; Barber, G.; Khouri, F.; Hempstead, A.; Larsen, M.; Olson, E.; Kelley, J.; Balch, G.; Caraher, J. Macromolecules 2002, 35, 5508.
39. Li, Q.; Jensen, J. O.; Savinell, R. F.; Bjerrum, N. J. Prog Polym Sci 2009, 34, 449.